

A Modeling Study to Determine the Effectiveness of an Energy Recovery Ventilator (ERV)

R. Pastor¹, E. Gutierrez-Miravete² and N. Lemcoff^{*,2}

¹General Dynamics Electric Boat, ²Rensselaer Polytechnic Institute Hartford

*Corresponding author: lemcon@rpi.edu

Abstract: The objective of this study is to numerically evaluate the effectiveness of an energy recovery ventilator (ERV) during the summer and winter seasons. An energy recovery ventilator is a new concept in ventilation systems that allows heat and mass transfer between two airstreams separated by a membrane. The effects of varying the following parameters were examined: flows through the supply and exhaust ducts, height of the exhaust channel, and diffusion coefficient through the membrane. The results showed that the countercurrent flow configuration is more effective than the concurrent flow configuration. For equal supply and exhaust channel flows, as the velocity decreases from 1.5 to 1 m/s, the effectiveness of the ERV increases from 0.51 to 0.61 and from 0.43 to 0.47, for the countercurrent and concurrent configurations, respectively.

Keywords: Energy Recovery Ventilator (ERV), Heat Transfer, Countercurrent Flow, Concurrent Flow, Ventilation

1. Introduction

In recent years, the need to conserve energy is receiving more attention. Therefore, there is a push in many engineering systems to use less energy, while maintaining the same functions and exceeding the performance required by earlier systems. This is the case for heating, ventilating, and air conditioning (HVAC) systems, that are required to provide comfort and quality air for occupants in buildings or offices, within reasonable installation, operation, and maintenance costs.

Using a traditional HVAC system for buildings that require high volume of outside air for heating and cooling will require more powerful ventilation systems to meet the buildings demands. This can be accomplished by using larger coils, fans, and/or heaters, but this would increase operating and equipment costs.

To reduce the energy consumption of ventilation systems, research in areas such as air-to-air energy recovery ventilator (ERV) or enthalpy exchanger is being carried out. The ERV takes advantage of the conditioned air that is normally exhausted out of the buildings, to either heat or cool (sensible heat) and humidify or dehumidify (latent heat) the incoming outside air. Therefore, this allows the ERV to be used during all the seasons. The heat and moisture transfer is possible because the water vapor-permeable membrane or plate, located between the conditioned and supplied air, allows the heat and moisture to pass through the membrane. The most common ERV design found in the market is the cross flow design, due to its simplified design, and the ease of duct sealing required for ERV systems. A depiction of a cross flow ERV design is shown in Figure 1. Due to the popularity of cross flow ERV systems, Zhang et al. [1] analyzed the heat and mass transfer in an ERV through the use of numerical analysis and conducting a test of a commercial product in a test lab. Min et al. [2] carried out a numerical analysis of the performance of ERVs by changing the membrane spacing and the thickness of the ventilator.

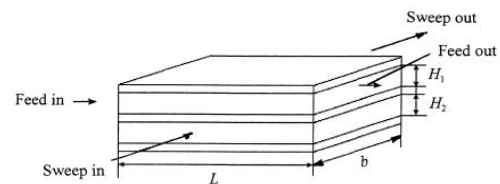


Figure 1. Schematic of a Cross-Flow Membrane ERV [1]

1.1 Problem Description

In this paper, the effectiveness of countercurrent and concurrent flows will be evaluated in a 2D domain. In the countercurrent flow membrane ERV, the exhaust and supply air flow in opposite direction, as shown in Figure 2.

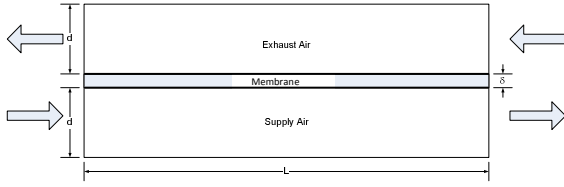


Figure 2. Schematic of a Countercurrent Flow Membrane ERV

In a concurrent flow membrane ERV, the exhaust and supply air flow in the same direction.

The studies will be carried out for both summer and winter conditions using COMSOL, a commercial software package [3].

2. Methodology

2.1 Physical Model

The ERV design is a core that contains alternate layers of membranes to separate and seal the exhaust and supply airstreams passages. Since the ERV has a symmetric design, the domain that will be evaluated will contain the membrane and only half of the channel volume of the supply and exhaust airstreams, as shown in Figure 2.

2.2 Mathematical Model

Based on the physical model described above, several assumptions will be made to assist in the modeling of the countercurrent and concurrent flow ERVs:

- Heat and mass transfer processes are in steady state.
- The physical properties of the air are constant.
- In the membrane, only heat conduction and water diffusion exists.
- Heat conductivity and water diffusivity in the membrane are constant.

2.2.1 Fluid Dynamics

The governing fluid dynamics equations for the ERV are the momentum transport equations and the equation of continuity for incompressible fluids:

$$\rho \frac{\partial u}{\partial t} - \nabla \cdot [\eta (\nabla u + (\nabla u)^T)] + \rho (u \cdot \nabla) u + \nabla p = F \quad (1)$$

$$\nabla \cdot u = 0 \quad (2)$$

where ρ is the density, η is the dynamic viscosity, u is the velocity field, p is the pressure, t is the time, and F is the volume force field. Assuming steady state and that the ERV flow is laminar and free of any force field, equation (1) simplifies to:

$$\eta \nabla^2 u + \rho (u \cdot \nabla) u + \nabla p = 0 \quad (3)$$

2.2.2 Heat Transfer

The governing heat transfer equation (conduction and convection) for the ERV is:

$$\delta_s \rho c_p \frac{\partial T}{\partial t} + \nabla \cdot (-k \nabla T) = Q - \rho c_p u \cdot \nabla T \quad (4)$$

where c_p is the heat capacity, k is the thermal conductivity, T is the temperature, δ_s is the time scaling coefficient, and Q is the heat source. Assuming steady state and no heat source in equation (4), the heat transfer equation simplifies to:

$$\nabla \cdot (-k \nabla T) = -\rho c_p u \cdot \nabla T \quad (5)$$

2.2.3 Mass Transfer

The governing mass transfer equation (diffusion and convection) for the ERV is shown below:

$$\delta_s \frac{\partial c}{\partial t} + \nabla \cdot (-D \nabla c + cu) = R \quad (6)$$

where c is the concentration, D is the diffusion coefficient, and R is the reaction rate. Assuming steady state and no reaction rate, equation (6) simplifies to:

$$\nabla \cdot (-D \nabla c + cu) = 0 \quad (7)$$

A pictorial description of the equations described above is shown in Figure 3.

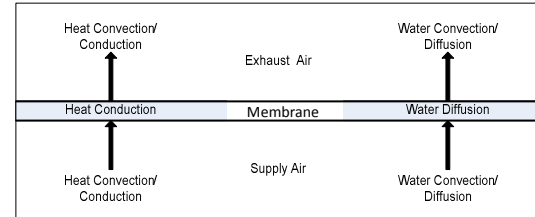


Figure 3. Pictorial Description of the Mathematical Model

2.2.4 Inlet Conditions

The inlet conditions for the countercurrent flow ERV are:

Supply Air:

$$u_s \Big|_{x=0} = u_{si} \quad (8)$$

$$T_s \Big|_{x=0} = T_{si}$$

$$c_s \Big|_{x=0} = c_{si}$$

Exhaust Air:

$$u_e \Big|_{x=L} = u_{ei} \quad (9)$$

$$T_e \Big|_{x=L} = T_{ei}$$

$$c_e \Big|_{x=L} = c_{ei}$$

where subscripts e , i , and s correspond to the exhaust, inlet, and supply, respectively. For concurrent flow, the same boundary conditions are used, except that for the exhaust flow the boundary is located at $x = 0$, in lieu of $x = L$.

2.2.5 Boundary Conditions

2.2.5.1 Fluid Dynamics

For the fluid dynamics, it will be assumed that the no slip condition exists at the membrane surface. At the system boundary of the ERV (the symmetry plane, at the center of the supply and exhaust channels) the following conditions exist:

$$u \cdot n = 0 \quad (10)$$

$$t \cdot (-pI + \eta \nabla u) n = 0 \quad (11)$$

which indicates no penetration and vanishing shear stresses. In equations (10) and (11), n indicates the normal vector, while t is the tangential vector.

At the outlet of the ERV it is assumed that Dirichlet condition exists for the pressure, and the viscous stress is small:

$$p = p_0 \quad (12)$$

$$(\eta \nabla u) n = 0 \quad (13)$$

2.2.5.2 Heat and Mass Transfer

Continuity of the heat flux is assumed at the membrane interfaces,

$$-n \cdot (q_1 - q_2) = 0 \quad (14)$$

where q is the heat flux.

At the symmetry plane, center of the supply and exhaust channels,

$$n \cdot (-k \nabla T) = 0 \quad (15)$$

At the outlet of the ERV, the boundary condition is a convective flux, where equation (15) is also valid.

It is also assumed that there is continuity of the mass flux at the membrane interfaces. Therefore, the boundary condition is

$$n \cdot (N_1 - N_2) = 0 \quad (16)$$

where N is the mass flux.

At the symmetry plane, center of the supply and exhaust channels, the boundary condition is

$$n \cdot (-D \nabla c + cu) = 0 \quad (17)$$

For the outlet of the ERV, the boundary condition is convective flux, namely

$$n \cdot (-D \nabla c) = 0 \quad (18)$$

2.2.6 Heat and Mass Transfer Effectiveness

The heat transfer effectiveness of the ERV is a way to measure its ability to transfer sensible and latent heat. In order to calculate the sensible heat transfer effectiveness, the change in sensible heat transfer of the supply and exhaust flows will be divided by twice the maximum sensible heat transfer possible for this system. The sensible heat transfer effectiveness is:

$$\varepsilon_s = \frac{\rho_s c_{ps} u_s d_s (T_{si} - T_{so}) + \rho_e c_{pe} u_e d_e (T_{eo} - T_{ei})}{2(\rho c_p u d)_{\min} (T_{si} - T_{ei})} \quad (19)$$

where the subscript o represents the outlet.

For the latent heat transfer effectiveness a similar approach to that described for the sensible heat transfer effectiveness will be used, except that the latent heat transfer is used in lieu of the sensible heat transfer. The equation for the latent effectiveness is:

$$\varepsilon_L = \frac{\rho_s u_s d_s (c_{si} - c_{so}) + \rho_e u_e d_e (c_{eo} - c_{ei})}{2(\rho u d)_{\min} (c_{si} - c_{ei})} \quad (20)$$

3. Finite Element Model

3.1 ERV Dimensions and Parameters

Based on the mathematical model described above, the COMSOL finite element software is used to model the ERV and analyze its capacity to transfer sensible and latent heat. The ERV basic dimensions were taken from [2] and are shown in Table 1.

Table 1. ERV Basic Dimensions

Length (mm)	250
Height (mm)	2
Membrane Height (mm)	0.1

The membrane properties were determined at the average inlet temperatures of the supply and exhaust streams. The remaining parameters for the membrane were obtained from [4]. The

diffusion and the thermal conductivity through the membrane were taken from Zhang [5]. Further details of this study can be found in Pastor [6]. The data described above is shown in Table 2.

Table 2. Membrane Properties and Parameters

	Summer	Winter
Inlet Dry Bulb Temperature (C)	29.500	11.350
Inlet Dry Bulb Temperature (K)	302.650	284.500
Inlet Wet Bulb Temperature (C)	21.500	7.300
Inlet Wet Bulb Temperature (K)	294.650	280.450
Density (kg/m ³)	1.160	1.240
Thermal Conductivity (W/m*K)	0.130	0.130
Diffusion (m ² /s) Membrane	8.000E-06	8.000E-06
Concentration (mol/m ³)	40.269	42.838
Diffusion (m ² /s) Air to H2O	2.680E-05	2.272E-05

Table 3. Supply Conditions and Properties for Summer and Winter Seasons

	Summer	Winter
Inlet Dry Bulb Temperature (C)	35.000	1.700
Inlet Dry Bulb Temperature (K)	308.150	274.850
Inlet Wet Bulb Temperature (C)	26.000	0.600
Inlet Wet Bulb Temperature (K)	299.150	273.750
Relative Humidity (%)	49.340	82.020
Pressure (mbar)	56.280	6.910
Density (kg/m ³)	1.145	1.284
Dynamic Viscosity (kg/m*s)	1.895E-05	1.738E-05
Thermal Conductivity (W/m*K)	0.026	0.024
Diffusion (m ² /s)	2.680E-05	2.120E-05
Concentration Air (mol/m ³)	39.550	44.342
Concentration Water (mol/m ³)	1.085	0.248

Table 4. Exhaust Conditions and Properties for Summer and Winter Seasons

	Summer	Winter
Exhaust Dry Bulb Temperature (C)	24.000	21.000
Exhaust Dry Bulb Temperature (K)	297.150	294.150
Exhaust Wet Bulb Temperature (C)	17.000	14.000
Exhaust Wet Bulb Temperature (K)	290.150	287.150
Relative Humidity (%)	49.590	45.866
Pressure (mbar)	29.850	24.877
Density (kg/m ³)	1.188	1.200
Dynamic Viscosity (kg/m*s)	1.844E-05	1.830E-05
Thermal Conductivity (W/m*K)	0.025	0.025
Diffusion (m ² /s)	2.484E-05	2.436E-05
Concentration Air (mol/m ³)	41.014	41.432
Concentration Water (mol/m ³)	0.600	0.467

The inlet conditions for the supply and exhaust streams for both the summer and winter seasons were obtained from [7]. The system properties required to solve the differential equations were obtained from [4] and [8]. The data is shown in Tables 3 and 4 for the supply and exhaust streams, respectively.

3.2 Fluid Dynamics

The initial stage of the finite element modeling is to solve the flow through the ERV

for both countercurrent and concurrent flows. The fluid dynamics model that was selected is the incompressible Navier-Stokes, steady state model in COMSOL. The velocity profiles obtained in this stage were used as input to model the heat and mass transfer in COMSOL.

3.3 Heat and Mass Transfer

For the heat transfer of the ERV, the conduction and convection, steady state model in COMSOL was used. The results from the heat transfer analysis will be used to calculate the sensible effectiveness of the ERV.

In the final stage of the analysis, the convection and diffusion steady-state model was selected in COMSOL and used to determine the ability of the ERV to humidify or dehumidify the air.

3.4 Meshing

To mesh the model, the mapped mesh parameter is used. This provides more flexibility and the user has better control in preventing the meshing of the model from exceeding the computer's memory. In order to solve the ERV in COMSOL, quadrilateral meshes were used, and were divided into equal spaces as defined in Table 5.

Table 2. Number of Elements

d	10
δ	10
L	200

4. Results

4.1 Problem Scenarios

In order to evaluate the effectiveness of the ERV, the velocities through both channels were varied between 1.0 and 1.5 m/s. The ERV is evaluated for both summer and winter conditions, and for each season the countercurrent and concurrent flow configuration is analyzed.

4.2 ERV Effectiveness with Equal Supply and Exhaust Flow

4.2.1 Summer Conditions

The sensible and latent effectiveness of the ERV were evaluated for the summer conditions using the data from Tables 1-4. The effectiveness of the ERV was calculated using equations (19) and (20). A summary of the results for the different supply and exhaust velocities for the summer conditions is shown in Table 6.

Table 3. Sensible and Latent Effectiveness with Equal Velocities (Summer)

Velocity (m/s)	Countercurrent ϵ_s	Concurrent ϵ_s	Countercurrent ϵ_L	Concurrent ϵ_L
1	0.605	0.474	0.609	0.478
1.25	0.553	0.451	0.555	0.456
1.5	0.509	0.427	0.511	0.433

It can be seen that, for both countercurrent and concurrent flow, the latent effectiveness of the ERV is nearly equal to the sensible effectiveness. This is because the diffusion coefficient in the membrane is relatively high and the control lies in the fluid phases. The results also show that, as the velocity decreases, the sensible and latent effectiveness of the ERV increase. This occurs because at slower velocities the residence time increases and a greater heat and mass transfer through the membrane is possible.

Plots for the sensible and latent effectiveness for the countercurrent and concurrent flow are shown in Figure 4 and 5, respectively.

It can be seen that for both sensible and latent effectiveness the countercurrent flow ERV is more effective than the concurrent flow configuration because the average driving force is higher. In the concurrent configuration, although the temperature and/or concentration differences at the inlet are quite high, they decrease rapidly and are very small at the channels exit.

To better understand the results for the sensible and latent effectiveness of the ERV, the temperature and concentration profiles for the ERV are analyzed. The results obtained for a channel flow of 1.25 m/s at various axial positions ($x = 0, 0.125, \text{ and } 0.250 \text{ m}$) are plotted as a function of the vertical distance. The plot of the temperature profiles are shown in Figures 6 and 7 for countercurrent and concurrent flow, respectively.

At the inlet of the supply channel the temperature is uniform and equal to 308.15 K. However, the temperature gradually decreases

through the membrane, and a larger temperature variation can be seen throughout the exhaust channel. The average temperature at the outlet of the exhaust channel is approximately 303 K.

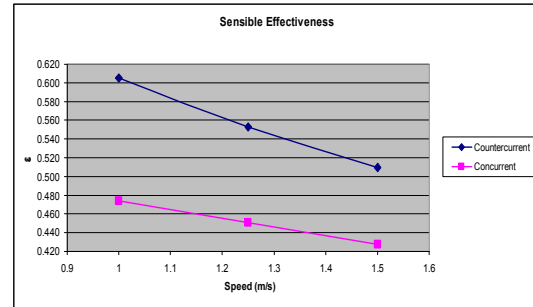


Figure 4. Summer Sensible Effectiveness for ERVs

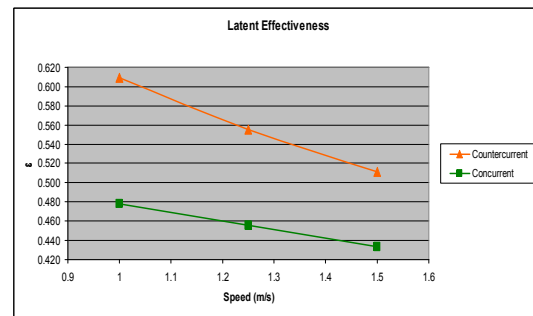


Figure 5. Summer Latent Effectiveness for ERVs

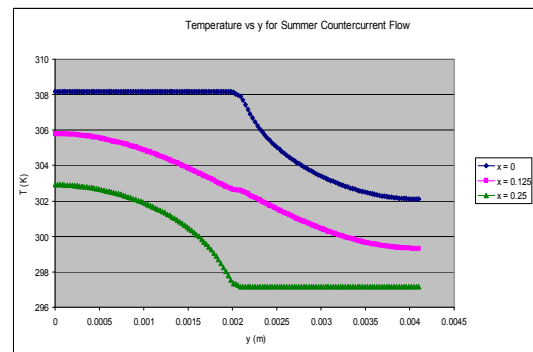


Figure 6. Countercurrent Flow Temperature Profile at Varying Channel Location

At the channel axial midpoint ($x = 0.125 \text{ m}$) the temperature gradually decreases from the bottom of the supply channel to the top of the exhaust channel. At the end of the ERV ($x = 0.250 \text{ m}$) a similar behavior to that at $x = 0 \text{ m}$ can be seen. The temperature at the exhaust inlet is uniform and equal to 297.15 K, while the average outlet temperature of the supply channel

is 302 K. It can be seen that the maximum temperature change occurs across the channel for the supply flow at $x = 0.250$ m, while for the exhaust flow it occurs at $x = 0$ m. Therefore, for the countercurrent flow, the temperature changes by approximately 6 K from the inlet to the outlet of the ERV, for both supply and exhaust flows.

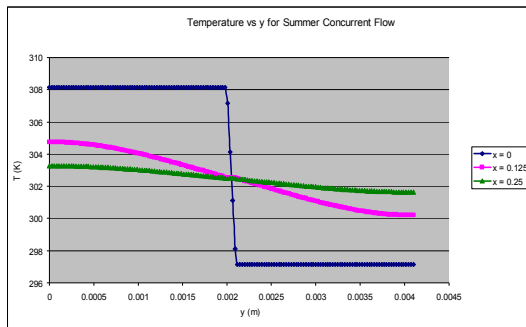


Figure 7. Concurrent Flow Temperature Profile at Varying Channel Location

For the concurrent flow, the temperature of the supply and exhaust streams at the inlet of the ERV ($x = 0$ m) is uniform. However, there is a large temperature variation across the membrane. The supply and exhaust inlet temperatures for the concurrent flow are identical to the countercurrent flow, namely 308.15 K and 297.15 K, respectively. At the channel axial midpoint, the behavior is the same as that described for the countercurrent flow. However, the temperature variation is not as steep. At the outlet of the ERV, the supply and exhaust average outlet temperatures are almost equal, namely 303 K and 302 K, respectively. For the concurrent flow, the temperature changes from inlet to outlet of the ERV by approximately 5 K, for both supply and exhaust flows.

The results for the concentration profiles for both countercurrent and concurrent flow are similar to those for the temperature profiles. Therefore, the countercurrent flow configuration is also more effective in mass transfer than the concurrent flow configuration.

4.2.2 Winter Conditions

The ERV performance at the winter conditions was evaluated through the same approach as that used for the summer conditions.

A summary of the results for the winter conditions is shown in Table 7.

Table 4. Sensible and Latent Effectiveness with Equal Velocities (Winter)

Velocity (m/s)	Countercurrent ϵ_S	Concurrent ϵ_S	Countercurrent ϵ_L	Concurrent ϵ_L
1	0.590	0.472	0.592	0.475
1.25	0.536	0.445	0.537	0.449
1.5	0.493	0.419	0.493	0.423

The results for the winter conditions shows that the effectiveness of the ERV for both countercurrent and concurrent configurations have a similar behavior as that described for the summer conditions. It is also observed that the sensible and latent effectiveness are slightly lower than that for the summer conditions. The sensible and latent effectiveness for the countercurrent and concurrent flow are plotted in Figures 8 and 9, respectively.

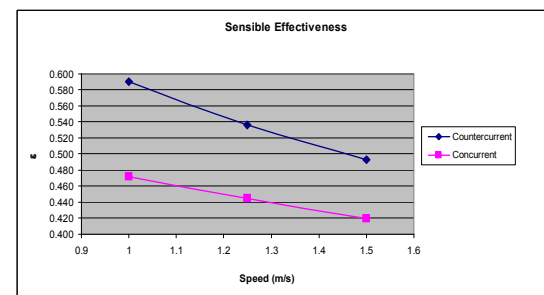


Figure 8. Winter Sensible Effectiveness for ERVs

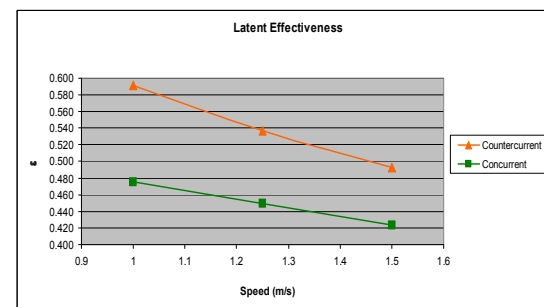


Figure 9. Winter Latent Effectiveness for ERVs

The plot shows that, for both sensible and latent effectiveness, the countercurrent flow ERV is more effective than the concurrent flow configuration, as it was observed for the summer conditions. The countercurrent and concurrent flow ERV temperature profiles at the channel axial midpoint as a function of the vertical distance, and at a speed of 1.25 m/s, for both summer and winter conditions, are shown in

Figure 10. For countercurrent flow, the maximum temperature difference across the channel is slightly greater than for the concurrent flow. This indicates that the heat transfer driving force for the countercurrent flow is greater, which leads to a higher sensible effectiveness.

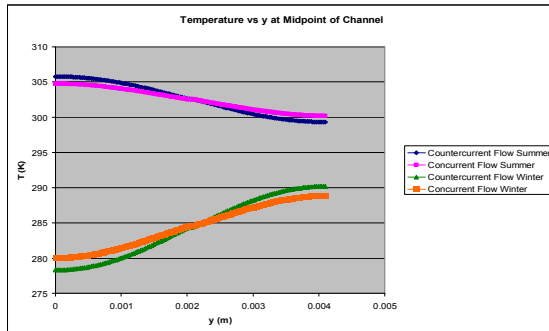


Figure 10. ERV Temperature Profile at $u = 1.25$ m/s

The corresponding concentration profiles are similar to the temperature profiles. This also indicates that the countercurrent flow is more effective than the concurrent flow configuration.

5. Conclusion

This paper shows that the countercurrent flow ERV is more effective than a concurrent flow ERV, and a higher overall temperature and/or concentration variation along the ERV is observed. It is also found that the countercurrent flow has the potential to greatly improve its effectiveness if the size of the ERV increases. However, for the concurrent flow the increase of the sensible and latent effectiveness cannot be achieved, because at the ERV outlet the supply and exhaust channels streams are almost in equilibrium.

The ERV effectiveness increases as the flow through the channel decreases because the air has more time to transfer heat and moisture from the supply to the exhaust channel or vice versa. Therefore, the temperature and concentration variations are much higher. So, in an ideal system, the velocity through an ERV should be reduced as much as possible to reduce the energy consumption and operating cost of an HVAC system. However, to process the same air flowrate a very large ERV system would be required. An optimum in the size and/or velocity will exist.

6. References

1. Zhang, L.Z.; Jiang, Y., Heat and mass transfer in a membrane-based energy recovery ventilator, Elsevier Ltd., *Journal of Membrane Science*, **163**, 29-38 (1999)
2. Min, Jingchun; Su, Ming, Performance analysis of a membrane-based energy recovery ventilator: Effects of membrane spacing and thickness on the ventilator performance, Elsevier Ltd., *Applied Thermal Engineering*, **30**, 991-997 (2010)
3. COMSOL AB, COMSOL Multiphysics Modeling Guide, COMSOL Version 3.5a, 1998-2008
4. Sugar Engineers, "Psychrometric Calculations", <http://www.sugartech.co.za/psychro/index.php>, November 16, 2010
5. Zhang, Li-Zhi, Heat and mass transfer in quasi-counter flow membrane-based total heat exchanger, Elsevier Ltd., *International Journal of Heat and Mass Transfer*, **53**, 547-548 (2010)
6. Pastor, Roy, A modeling study to determine the effectiveness of an Energy Recovery Ventilator (ERV), Master's Project, Rensselaer Polytechnic Institute, 2010
7. Air Conditioning, Heating, and Refrigeration Institute (AHRI), ANSI/AHRI Standard 1060 - 2005 Standard for Performance Rating of Air-to-Air Exchangers for Energy Recovery Ventilation, 2005
8. Cengel, Yunus A., Heat and Mass Transfer A Practical Approach, Third Edition, McGraw-Hill Companies, New York, 2007, pp. 782 and 860

7. Acknowledgements

One of the authors (R.P.) wants to thank his wife for support in his life and future endeavors, Professors Norberto Lemcoff and Ernesto Gutierrez-Miravete for their assistance and guidance in completing this paper, and Electric Boat and Rensselaer Polytechnic Institute for providing the opportunity to share his work in the conference.